The dual source region for the 2004 Sumatra tsunami

Isaac V. Fine,[1,2] Alexander B. Rabinovich,[1,3] and Richard E. Thomson[1]

Received 16 May 2005; revised 24 June 2005; accepted 18 July 2005; published 18 August 2005.

[1] Wave arrival times obtained from coastal tide gage and satellite altimetry records for the Indian Ocean are used to delineate the source region for the December 26, 2004 Sumatra tsunami. Findings define a curved, 250-km wide, 1000-km long tsunami source region centered over the Sunda Subduction Zone, which closely matches the seismic source estimated from broadband geophysical data. Imbedded in this general region are "hot spots" associated with the southern fast-slip and northern slow-slip domains which served as distinct source areas for the destructive waves that inundated the coast of the Indian Ocean. **Citation:** Fine, I. V., A. B. Rabinovich, and R. E. Thomson (2005), The dual source region for the 2004 Sumatra tsunami, *Geophys. Res. Lett.*, *32*, L16602, doi:10.1029/2005GL023521.

1. Introduction

[2] The Sumatra-Andaman Island megathrust earthquake of 00:59 UTC 26 December 2004 was first estimated as $M_w = 9.0$ and later upgraded to $M_w = 9.3$ based on analysis of the normal modes of the Earth [*Stein and Okal*, 2005]. This was the second largest earthquake ever recorded. Tsunami waves generated by the earthquake were responsible for over 250,000 dead and missing, and left millions homeless and displaced in areas bordering the Indian Ocean.

[3] Tsunami records from a number of tide gages in the Indian Ocean [*Merrifield et al.*, 2005] are of sufficiently high quality and resolution for accurate estimation of tsunami arrival times. The tsunami was also recorded by the Jason-1 and Topex/Poseidon satellites [*Gower*, 2005; *Smith et al.*, 2005]. Data from the Eastern and Central Indian Ocean, which are close to the source area, are critical for examination of the event and its regional impact. In this study, we use inverse wave-tracing to delineate the generation region for the Sumatra tsunami. Results are based on tsunami arrival times from tide gage and satellite altimetry records and on wave propagation speeds derived using high resolution 1-min (1.85 km) bathymetric data.

2. Observations

[4] Digital tsunami records were obtained from the University of Hawai'i Sea Level Center database (http://ilikai.soest.hawaii.edu/uhslc/iotd) for five tide gage stations (Colombo, Hanimaadhoo (2-min sampling), Male, Gan (4-min), and Diego Garcia (6-min) [*Merrifield et al.*, 2005]) and from the National Tidal Centre, Australian Bureau of Meteorology for the Cocos Islands (1-min). Tsunami wave plots and supporting information for three stations on the east coast of India (Vishakhapatnam, Chennai, Tuticorin) are from a National Institute of Oceanography report (available at http://www.nio.org/jsp/tsunami.jsp). We also used a wave height time series collected by the "fishfinder" (depth sounder) on the yacht "Mercator", anchored near the coast of Phuket (Thailand) (T. Siffer, "Mercator" depth gage recording of 26 December 2004 tsunami, available at http://www.knmi.nl/seismologie/) (Figure 1). Measurements from tide gauge stations on the coasts of Thailand and Indonesia were not used because of their inadequate resolution of tsunami arrival times.

[5] Altimetry measurements of the Sumatra tsunami (the first major tsunami recorded by orbiting satellites) were obtained from the Jason-1 and Topex/Poseidon satellites [*Smith et al.*, 2005] as they transited the Indian Ocean about 150 km apart approximately two hours after the quake. As indicated by Figure 1, the tracks crossed the spreading front of the tsunami waves twice: in the north in the Bay of Bengal and in the south about 1200 km southward from Sri Lanka. In addition to augmenting the overall data coverage, the satellite data yield snapshots of the spatial structure of the tsunami waves for the open Indian Ocean for which there are no sea level recorders.

3. Inverse Wave-Tracing

[6] Following [*Abe*, 1973; *Satake*, 1993], we used inverse wave-tracing (wave-retracing) to determine the source regions for the leading edge of the tsunami. For

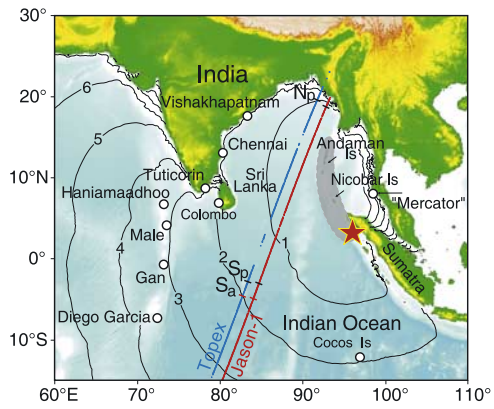

Figure 1. Location of tide gages in the Central and East Indian Ocean. The blue and red lines show the tracks of the Topex/Poseidon and Jason-1 satellites that passed over the Indian Ocean about two hours after the December 26, 2004 earthquake. The red star marks the earthquake epicenter; the shaded gray area bordered by a dashed line specifies the aftershock region. The gray lines are calculated hourly isochrones of tsunami travel time.

[1]Department of Fisheries and Oceans, Institute of Ocean Sciences, Sidney, British Columbia, Canada.
[2]Heat and Mass Transfer Institute, Minsk, Belarus.
[3]Shirshov Institute of Oceanology, Moscow, Russia.

0094-8276/05/2005GL023521$05.00

Table 1. Tsunami Properties Estimated From Coastal Tide Gage Records in the Indian Ocean

No.	Station	Country	Coordinates	First Arrival		First Crest	
				Arrival, UTC	Travel Time	Arrival, UTC	Travel Time
1	Vishakhapatnam	India	17.65°N; 83.28°E	03:35	2hr 36min	03:50[a]	2hr 51min
2	Chennai	India	13.10°N; 80.32°E	03:35	2hr 36min	03:44[a]	2hr 45min
3	Tuticorin	India	08.75°N; 78.20°E	04:27	3hr 28min	04:41[a]	3hr 42min
4	Colombo	Sri Lanka	06.93°N; 79.83°E	03:49	2hr 50min	03:58	2hr 59min
5	Hanimaadhoo	Maldives	06.77°N; 73.18°E	04:31	3hr 32min	04:39	3hr 40min
6	Male	Maldives	04.18°N; 73.52°E	04:14	3hr 15min	04:24	3hr 25min
7	Gan	Maldives	00.68°S; 73.17°E	04:18	3hr 19min	04:32	3hr 33min
8	Diego Garcia	UK	07.30°S; 72.38°E	04:45	3hr 46min	04:54	3hr 55min
9	Cocos	Australia	12.13°S; 96.88°E	03:20	2hr 21min	03:26	2hr 27min
10	Yacht "Mercator"	Thailand	07.75°N; 98.28°E	02:38	1hr 39min	02:54	1hr 55min

[a]Estimated from tsunami time series plots.

each site, we estimated the observed propagation time from the beginning of the earthquake to the arrival at the recording site (Table 1). Source delineation is limited by the accuracy of the estimated arrival times, by the bathymetry data used in the numerical simulations (1-min GEBCO topographic data [*British Oceanographic Data Centre*, 2003]), and by non-linear and dispersive effects. As shown in Figure 2a, the aftershock region following the December 26, 2004 Sumatra Earthquake extends from 2° N to 15° N along the Indo-Andaman plate boundary. Although there have been several major thrust earthquakes in this region in the past, the M_w = 9.3 earthquake of December 2004 has no historical precedent [*Bilham et al.*, 2005]. The distribution of aftershocks indicates that the primary rupture accompanying the main shock took roughly 10 min to propagate 1300 km northward from the epicenter near 3.3° N, corresponding to an average northward propagation speed of ~2 km·s^{-1} [*Stein and Okal*, 2005].

[7] The stations used in our first-wave arrival time analysis fall into four groups (Table 1): "northwestern" (stations 1–2); "western" (3–8); "southern" (9); and "eastern" (10). The first waves to arrive at gages in the western group followed similar wave paths (Figure 2a). As a consequence, computed inverse wavefront contours closely parallel one another, thereby defining approximately the same western boundary for the source region. Spatial separations are within the errors of our simulations (inaccuracies in the estimated arrival times are about 4–6 min). For all six sites, intersection points for the leading wave-front curves are co-located above the Sumatra Trench

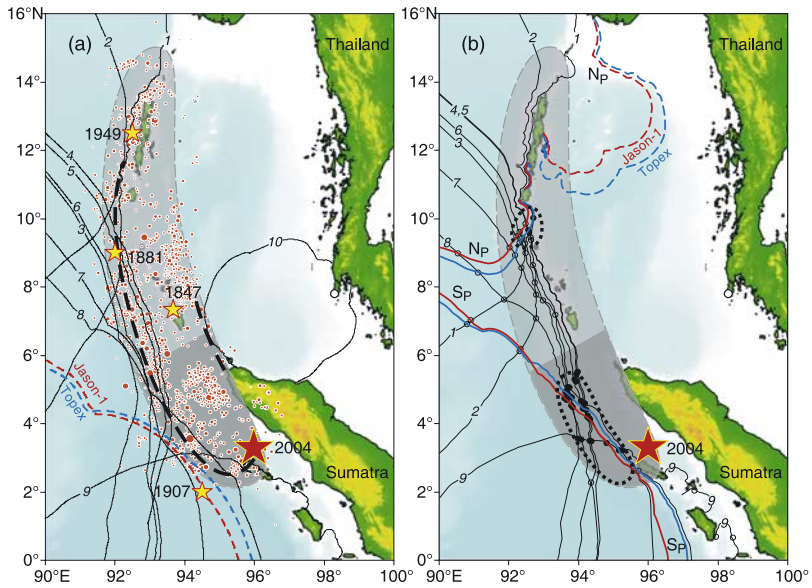

Figure 2. (a) Aftershocks observed in the Nicobar-Andaman islands region for a month following the December 26, 2004 earthquake. The red star marks the earthquake epicenter; smaller yellow stars show major historical earthquakes, red circles indicate aftershock positions. The shaded gray region denotes the general source region for the Sumatra tsunami; the darker portion of the gray zone is the fast slip area estimated from body waves [*Stein and Okal*, 2005]. Solid black lines represent the inverse wave propagation contours derived from the first wave arrival times for tide gages (numbers refer to stations listed in Table 1), while blue (solid) and red (dashed) lines are for Topex/Poseidon and Jason-1 altimetry records (S_a). (b) The inverse travel-time contours obtained for peak waves measured by tide gages (black solid lines) and by Topex/Poseidon and Jason-1 satellites (blue and red solid lines marked S_p and N_p). The thick black dotted lines denote the calculated source regions for the peak tsunami waves. Circles identify line crossings inside (solid) and outside (open) the southern and northern tsunami source areas.

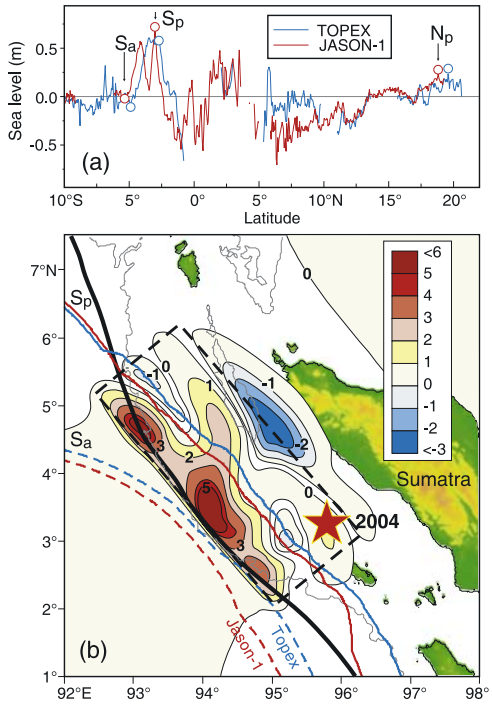

Figure 3. (a) Topex/Poseidon and Jason-1 altimetry profiles for the Indian Ocean. Empty circles indicate positions of the leading south wave (S_a), first south peak (S_p), and first north peak (N_p). Elevations have been corrected for background oceanic features. (b) Contours of the earthquake surface displacements (in meters) for the vertical component of motion [from *Ji*, 2005] along with the calculated inverse travel-time contours for the peak waves from the satellite tracks. The solid blue and red lines were derived using peak waves on the southern (S_p) portion of the altimetry profiles; the dashed lines are the corresponding inverse first arrival contours for S_a. The thick black solid line denotes the plate boundary and the dashed box the principal earthquake zone.

in the area between 4° and 5° N, in close proximity to the "main source" region [*Bilham et al.*, 2005; *Stein and Okal*, 2005].

[8] Wave-retracing based on the tide gage station in the Cocos Islands (9) locates the southern boundary of the source, with the tsunami wavefront coincident with the southern edge of the aftershock region (Figure 2a). The northwestern stations Vishipanatam (1) and Chennai (2), on the east coast of India, help define the long-axis extent of the tsunami source. Following corrections for delays due to the finite rupture speed of 2 km·s^{-1} and nonlinear effects on wave propagation speed for the shallow-water region off the eastern coast of India, wave-retracing confirms that the northernmost end of the source region extended to at least 10–11°N, consistent with recent estimates based on analysis of the earthquake-induced eigenoscillations [*Stein and Okal*, 2005], Global Positioning System (GPS) measurements [*Vigny et al.*, 2005], and hydroacoustic data (J. A. Guilbert et al., An original image of the seismic rupture of the Sumatra *Mw* = 9.0 using PMCC from seismic and hydroacoustic small array, submitted to *Geophysical Research Letters*, 2005, hereinafter referred to as Guilbert et al., submitted manuscript, 2005).

[9] The first recorded waves at stations 1–9 were crests (positive waves) due to a rapid uplift on the western side of the source area. In contrast, the first waves recorded on the coasts of Thailand and Indonesia were troughs (negative waves), indicating an abrupt subsidence on the eastern side of the source region. Because of the relatively poor resolution of gages in Thailand and Indonesia, the only reliable estimate for the arrival times in this region is from the sounder on the yacht "Mercator." According to this record, the calculated inverse-wave front (10) for the leading tsunami wave coincides with the border of the aftershock zone extending northward from the Island of Sumatra.

[10] As with the tide gage records for stations 1–9, the leading wave measured by satellite (Figure 3a) was a ~50 cm high wave crest (corrected for more persistent oceanic features such as eddies using altimeter data from the tracks before and after the event [*Smith et al.*, 2005]). Using the times and positions for the leading edge of the first "south" wave (S_a) along the satellite tracks (Table 2), inverse wave tracing yields contours which generally coincide with one another and with contours calculated from tide gage data. These results position the southwestern border of the source region close to the main shock epicenter (Figure 2a).

[11] Locating the northern boundary of the source region proved more problematic. The leading edge of the advancing tsunami cannot be precisely pinpointed along the northern sections of the satellite tracks because the lead wave struck the coast a few minutes before the satellites passed over (Figure 1). Consequently, we have had to turn to the arrival times for the first wave crest (Table 2), which identifies the source region for the maximum tsunami waves. As illustrated in Figure 3a, the "northern" peak in the Jason-1 and Topex/Poseidon records had a height of ~40 cm. According to Figure 2b, the inverse tsunami travel-time lines for the northern peak (N_p) pass through the northern part of the rupture zone between 9° to 13°N. The eastern part of this particular zone cannot be the source for this peak because it was a subsidence region, and we can exclude the Andaman Islands because tsunamis are not generated on land. Therefore, the source region for this

Table 2. Tsunami Properties Estimated From the Jason-1 and Topex/Poseidon Satellite Tracks

	Jason-1			Topex/Poseidon		
Wave Parameters	Coordinates	Arrival, UTC	Travel Time	Coordinates	Arrival, UTC	Travel Time
			South			
First arrival	04.91°S; 84.00°E	02:54	1hr 55min	04.56°S; 82.70°E	03:00	2hr 01min
First crest	03.01°S; 84.68°E	02:54	1hr 55min	02.80°S; 83.34°E	03:01	2hr 02min
			North			
First crest	18.81°S; 92.80°E	03:02	2hr 03min	19.59°S; 91.70°E	03:09	2hr 10min

peak wave must have been located to the south of the Andaman Islands, between 9.0° to 10.2°N, about 600–700 km north of the earthquake epicenter (3.3°N). We note that, if the leading edge of the satellite-detected tsunami was actually that of the leading wave immediately after reflection from the Myanmar coast, the northern source region would need to be extended even further to the north.

[12] Wave-retracing based on the southern satellite altimetry peak (S_p) yields inverse contours that pass through the southern part of the aftershock area from NW to SE (Figure 3b). The resulting inverse propagation contours derived from the two satellite tracks are mutually consistent. They fall close to the plate boundary and agree well with the source of the principal tsunami defined by *Bilham et al.* [2005]. A comprehensive analysis of this area based on IRIS teleseismic data [*Ji*, 2005] shows that the rupture for 2004 event was along several fault segments with different strikes (Figure 3b). The source boundary locations calculated from the S_p satellite positions agree well with model results [*Ji*, 2005], and closely coincide with the maximum (~5 m) uplift zones. The small differences in positioning are bounded by the ±3 min confidence interval in the wave arrival times (Figure 3b).

4. Discussion

[13] As illustrated in Figure 2a, wave re-tracing based on the initial tsunami arrival times defines the general source region for the 2004 Sumatra tsunami as a curved, 250-km wide, roughly 1000-km long earthquake rupture segment centered over the Sunda Subduction Zone. The next step was to identify locations of more localized, imbedded source areas responsible for the major wave destruction in the Indian Ocean. The re-traced wave fronts from the peak-wave satellite track position S_p (Table 2) and from the peak-wave arrival contours (Figure 2b) estimated from the western (3–8) group of tide gages intersect at approximately 4.5°N, 94°E (Figure 3b), identifying this as the likely generation region for the destructive tsunami waves. This result is supported by the peak contour derived for the Cocos Islands (9) which intersects peak contours for stations 3–8 and S_p at 3°N, between 94° and 95°E (Figure 2b). On the other hand, this southern tsunami source region cannot be responsible for the northern satellite peak wave (N_p) that was observed by the two satellites, nor for the first waves that arrived at tide gages 1 and 2 along the east coast of India. These smaller leading waves clearly point to a second, albeit less intense, "northern" tsunami source region.

[14] In summary, the tide gage (Table 1) and satellite (Table 2) data reveal two well-defined zones that include most of the crossings (the most probable source areas) of the inverse wave-propagation fronts for wave crests: (1) a "southern source" located west of North Sumatra (2.5°–5.3°N), close to the main epicenter; and (2) a "northern source" immediately to the south of the Andaman Islands (9.0°–10.2°N). This "dual source" concept is supported by estimates of the surface deformation measured in this region by GPS [*Vigny et al.*, 2005] and by independent conclusions provided by analyses of hydroacoustic and low-frequency seismic information from two small research arrays in Diego Garcia and Thailand (Guilbert et al., submitted manuscript, 2005). The southern source region is coincident with the "fast slip" area estimated from body waves [*Stein and Okal*, 2005; *Ji*, 2005]. According to our computations, this zone is responsible for the generation of the major tsunami waves that struck Sri Lanka, the Maldives and the coasts of East and South Africa. These also are the dominant waves that propagated throughout the world ocean, reaching such distant locations as Halifax in the North Atlantic and the Aleutian Islands in the North Pacific. The "peak" source (marked by thick dotted line in Figure 2b) had a spatial extent of about 350 km. When findings for the leading waves are included, the entire southern source is estimated to be 600–650 km long, in agreement with seismological estimates [*Stein and Okal*, 2005; *Bilham et al.*, 2005; *Ji*, 2005].

[15] The northern tsunami source region coincides with the area of slow slip [*Stein and Okal*, 2005]. This weaker source region was responsible for the somewhat smaller first waves that reached the coasts of Bangladesh, Myanmar, and eastern India. When both segments are combined, the tsunami source region derived from the first-wave arrival times (marked by a solid dashed line in Figure 2a) is more than 1000 km long. It was because of this large spatial extent that low frequency wave components were so prevalent in the tsunami waves recorded throughout the world ocean.

[16] **Acknowledgments.** We thank the Sea Level Center, University of Hawaii and the National Tidal Centre, Australian Bureau of Meteorology, for providing the sea level data used in this study. We also thank Kelin Wang, Pacific Geoscience Centre, Sidney, BC for discussions on earthquake aftershocks and Patricia Kimber for drafting the figures. Constructive comments from the two reviewers are gratefully acknowledged.

References

Abe, K. (1973), Tsunami and mechanism of great earthquakes, *Phys. Earth Planet. Inter.*, *7*, 143–153.

Bilham, R., E. R. Engdahl, N. Feldl, and S. P. Satyabala (2005), Partial and complete rupture of the Indo-Andaman Plate boundary, 1847–2004, *Seismol. Res. Lett.*, in press.

British Oceanographic Data Centre (2003), *GEBCO Digital Atlas*, Natl. Environ. Res. Counc., Swindon, U. K.

Gower, J. (2005), Jason-1 detects the December 26 2004 tsunami, *Eos Trans. AGU*, *86*(4), 37–38.

Ji, C. (2005), Magnitude 9.0 earthquake off the west coast of northern Sumatra: Preliminary rupture model, report, U.S. Geol. Surv., Denver, Colo. (Available at http://neic.usgs.gov/neis/eq_depot/2004/eq_041226/neic_slav_ff.html)

Merrifield, M. A., et al. (2005), Tide gage observations of the Indian Ocean tsunami, December 26, 2004, *Geophys. Res. Lett.*, *32*, L09603, doi:10.1029/2005GL022610.

Satake, K. (1993), Depth distribution of coseismic slip along the Nankai Trough, Japan, from joint inversion of geodetic and tsunami data, *J. Geophys. Res.*, *98*(B3), 4553–4565.

Smith, W., R. Scharroo, V. Titov, D. Arcas, and B. Arbic (2005), Satellite altimeters measure Tsunami, *Oceanography*, *18*(2), 10–12.

Stein, S., and E. A. Okal (2005), Speed and size of the Sumatra earthquake, *Nature*, *434*, 581–582.

Vigny, C., et al. (2005), Monitoring of the December 26th megathrust earthquake in SE Asia by GPS, paper presented at European Geosciences Union General Assembly, Vienna.

I. V. Fine, A. B. Rabinovich, and R. E. Thomson, Department of Fisheries and Oceans, Institute of Ocean Sciences, 9860 West Saanich Road, Sidney, BC, Canada, V8L 4B2. (thomsonr@pac.dfo-mpo.gc.ca)